FEASIBILTY ANALYSIS OF SHRINK FLANGING PROCESS WITH SUPPORT OF NUMERICAL SIMULATION

Constantin DRAGHICI [1]

The article presents scientifically results of the numerical simulation experimental works accomplished by the author for shrink flanging process regarding feasibility and thickening of the side walls obtained by shrink flanging process. The research purpose is to achieve a numerical model and determining a relation for estimating the thickening of the side walls obtained by shrink flanging process by mathematical modeling using response surface method considering six geometrical characteristics of the part.

Keywords: shrink flanging process, thickening, finite element method, feasibility, forming limit diagram, response surface method

1. Introduction

In the automotive industry, most companies use numerical simulation software for evaluation of the cold plastic deformation processes of the parts obtained from sheet metal and for analysis of their feasibility. These programs are based on practical experience, industrial knowledge and expertise in sheet metal forming. With its support, it is possible to find different solution for every situation and also to analyze and optimize the cold plastic deformation processes [1]. Some of the factors that influence feasibility of the parts are geometrical characteristics of their mechanical properties of sheet material used, geometry of forming punch, material thinning, material thickening and respective, friction conditions.

Material thickening is very important in production of quality stamped products. Also, the material's Forming Limit Curve (FLC) offers important information about the material's formability. This paper presents numerical simulation of the shrink flanging process, a numerical tool and results obtained about the influence of geometrical characteristics of the flanged parts regarding feasibility, shrink flanging prediction in sheet material forming and thickening, obtained model, statistical analysis and graphics in shrink flange forming. There are presented also some observations and conclusions regarding the obtained results.

[1] PhD., Eng., Lecturer, Dept. of Theory of Mechanisms and Robots, University POLITEHNICA of Bucharest, Romania, e-mail: ctin_draghici@yahoo.com

The purpose of this study is statistical modelling of the thickening as a function of the six geometrical parameters: fillet radius from horizontal plane, fillet radius from vertical plane, connection angle between the lateral side walls, bend angle between the left hand side wall of the part and normal to the surface of the part, bend angle between the right hand side wall of the part and normal to the surface of the part, and wide of the flanged wall, figure 1.

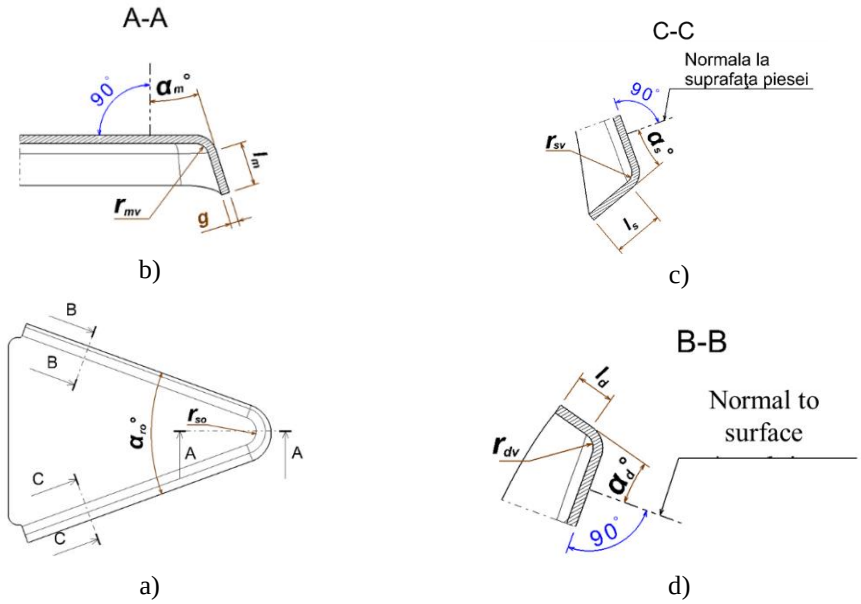

Fig. 1. Geometrical parameters of forming flange process

where:

r_{so} - fillet radius in horizontal plane, (mm);
$\propto^{\circ}_{ro}$- connection angle between the lateral side walls, (degree)
$\propto^{\circ}_{m}$ - medium bend angle between the side wall of the part and normal to the surface of the part, (degree)
r_m - medium fillet radius in vertical plane, (mm)
l_m - length of the medium flanged wall, (mm).
$\propto^{\circ}_{d}$ - bend angle between the right hand side wall of the part and normal to the surface of the part, (degree),
r_{dv} - right hand fillet radius in vertical plane, (mm)
l_d - length of the right hand flanged wall, (mm);
$\propto^{\circ}_{s}$ - bend angle between the left hand side wall of the part and normal to the surface of the part, (degree);
r_{sv} - left hand fillet radius in vertical plane, (mm);

l_s - length of the left hand flanged wall, (mm).

Finite element method is used in order to perform this numerical tool. Using this software's have resulted in major cuts of costs for the design dies, the possibility to test various technical solutions or test new innovative solutions, respectively, predict accurately the risk of defects in parts during forming processes and completely eliminating of tests laboratory [1].

In this study, simulations correspond to the following real working conditions of a car press lines factory:

- material thickness, g - 0.65 mm;
- radius of flanging punch - 2 mm;
- imported digitized surface corresponds to the inner surface of the piece;
- press stroke - 700 mm;
- cushion stroke - 350 mm;
- the value of the force for restraining of the blank with the pad applied to keep the sheet sample to remain fixed between die and pad was 10000 kN
- coefficient of friction - 0.16. This corresponds to a minimum friction resulting from the existence of a protective solution coatings against oxidation blanks, coverage provided by the supplier of cold rolled sheet metal;
- the deviation from the contour of the final part does not exceed 0.15 mm.

Shrink flanging, figure 2, is one form of flanging. Each radial zone (shaded region) is folded 90° along a radial line to form the flange or wall. Since the arc length of the final flange or wall is smaller than the arc length of the element from which it was formed, compression must take place in the circumferential direction. The greater the flange depth, the greater is the amount of compression. In addition, the compression is largest at the top of the flange and is zero at the flange radius [2].

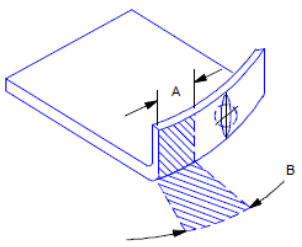

Fig. 2. Shrink flanging

For the flanged parts to fulfill its functional role, they must accomplish the following conditions:

- the resulting wall height must be as high as possible or minimum, respectively: 2,5 x thickness;
- the thickening of the wall cannot exceed maximum admissible value accepted, respectively: 1% of the thickness of the part;
- the edges of the shrink flanged parts must be smooth and free of cracks

Shrink flange forming is used to obtain a lot of parts, especially for the parts .form automotive industry, like fenders, doors, auto body chase and other, figure 3.

a) parts with visual impact (exterior parts)

b) structure parts

Fig. 3. Samples of shrink flanged parts

In literature, one method for feasibility evaluation of the shrink flange forming, figure 4, is presented in [3, 4, 5 and others]. Evaluation is made with the help of flange ratio, k_1, equation 1, taking in account two geometrical characteristics, respectively, cut radius, R, and wide of the flange, h, [3, 4, 5].

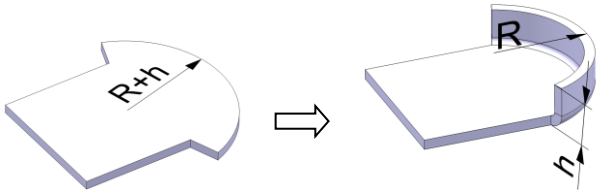

Specimen Part

Fig. 4. Flanged part

The value of this coefficient, k_1, must be greater than a recommended limit value indicated in literature, k = (0,8…0,9), [3, 4, 5]. If the value of this coefficient is smaller than recommended limit value, the shrink flange forming is made in two or more operations.

$$k_1 = \frac{R}{R+h} \tag{1}$$

Other authors use a chart for calculating widths of open or closed flanges, [6]. Also, there are some studies regarding the study of stretch flanging process with support of finite element analysis presented by [7]. In those studies, was shown that the geometrical parameters have greater influence upon the formability of shrink flanging process as compared to material parameters.

2. FEM simulation setup

In this study, a commercial software was used as the FEM simulation tool, respectively, AutoForm, which is one of the best and most widely used solution in the world for analysis of parts feasibility.

The numerical model is presented in figure 5 and it consists in 3 rigid (punch, die and blank holder) and one deformable (specimen) bodies. The cinematics of the flanging is presented in figure 6.

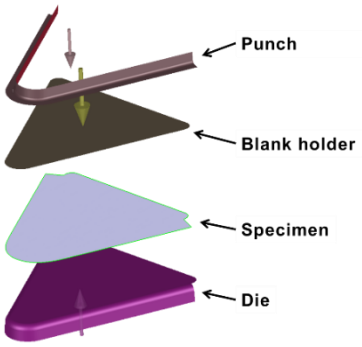

Fig. 5. Numerical model

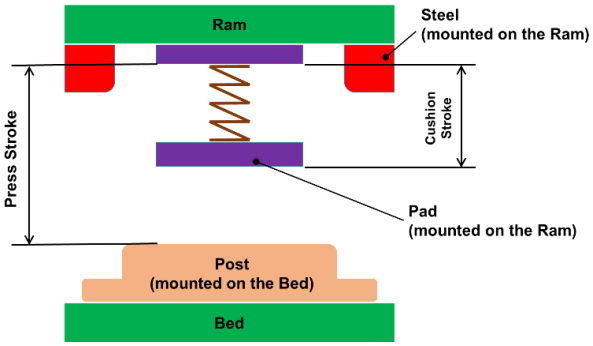

Fig. 6. Tool kinematic

Analyzing geometrical characteristics which have influence on shrink flanging process, figure 1, numerical simulation was made taking in account six geometrical parameters. These, and the levels of the experimental data for assessing the feasibility of the shrink flanged parts are presented in table 1.

The simulation of shrink flanging process has been carried out for a commercially-available cold rolled sheet metal DC04 with thickness of 0.65 mm. DC04 is a low carbon steel with typical applications in die forming, small and medium scale deep drawing and production of specially deep drawn and complex parts. Values of mechanical properties and chemical compositions of this sheet metal according to European norm EN 10130 are presented in table 2 [10].

Table 1

The variation level of the experimental used

Natural variables	*Level* / *Cod.*	*Codified*				
		-2	*-1*	*0*	*+1*	*+2*
		Variation levels, in natural units				
fillet radius in horizontal plane, r_{so} (mm)	x_1	1·g	9,65·g	15,5·g	21,35·g	30·g
fillet radius in vertical plane, r_v (mm)	x_2	1,5·g	4·g	5,75·g	7,5·g	10·g
connection angle between the lateral side walls, $\propto^{\circ}_{ro}$ (degree)	x_3	10	34	50	66	90
bend angle between the left hand side wall of the part and normal to the surface of the part, $\propto^{\circ}_{s}$ (degree)	x_4	0	3	5	7	10
bend angle between the right hand side wall of the part and normal to the surface of the part, $\propto^{\circ}_{d}$ (degree)	x_5	0	3	5	7	10
wide of the flanged wall, l (mm)	x_6	1·g	3,69·g	5,5·g	7,31xg	10·g

where: g - thickness of the part

Table 2

Values of mechanical properties of DC04 Am sheet metal

EN 10130	**Yield Point $R_{p0,2}$ [MPa]**	**Tensile strength, R_m [MPa]**	**Fracture elongation, A_{80} [%]**	**Vertical anisotropy, r_{90} min**	**Work hardening exponent, n_{90} min**	**Chemical composition [max. %]**					
						C	**Mn**	**P**	**S**	**Si**	**Al**
DC04	210	270 - 350	38	1.6	0.18	0.08	0.40	0.025	0.025	0.025	0.020

3. Determining the dependent variables

Analyzing the steps of the shrink flanging process between the top dead center (TDC) and bottom dead center (BDC) of the press, figure 7 (a, b, c, d, e, f), there was considered as dependent variables process the admissible thickening and feasibility, table 3. Also, for checking feasibility it was used Forming Limit Diagram (FLD), figure 8.

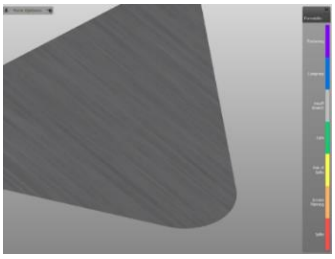

Fig. 7.a. Shrink flanging process analysis - start of the press stroke

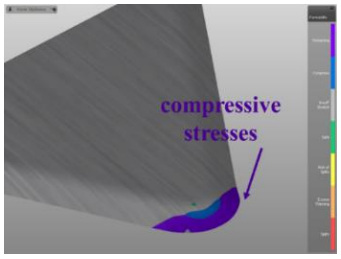

Fig. 7.b. Shrink flanging process analysis - 10 mm before bottoming

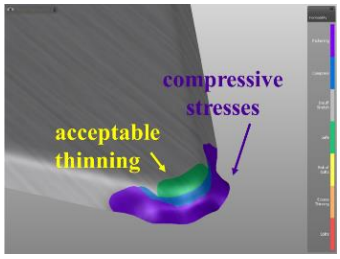

Fig. 7.c. Shrink flanging process analysis - 7 mm before bottoming

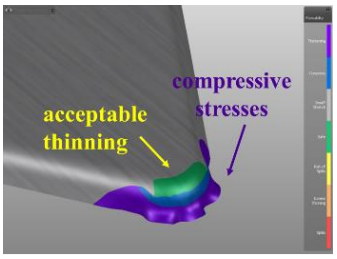

Fig. 7.d. Shrink flanging process analysis - 5 mm before bottoming

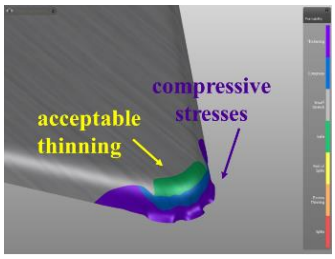

Fig. 7.e. Shrink flanging process analysis - 3.5 mm before bottoming

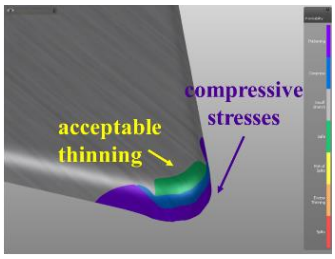

Fig. 7.f. Shrink flanging process analysis - bottoming (end of press stroke)

Table 3

Dependent variables of shrink flanging process

No. crt.	Dependent variables	U.M.
1	Admissible thickening	%
2	Formability	-

From the analysis of the deformation process, figures 7 and 8, it can be seen as the most significant parameters are thickening of the side walls and feasibility of the part.

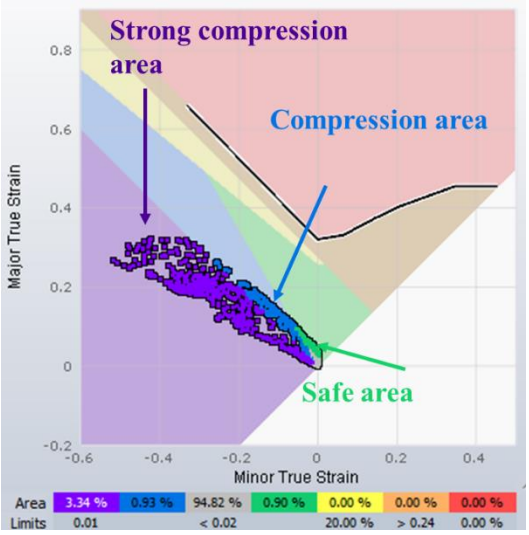

Fig. 8. Forming Limit Diagram

4. Shrink flanging process model and influence of considered parameters on shrink flanged process

For a more rigorous emphasis of the influence of the deformation process on the thickening and feasibility, as well to define the process optimizing, the process analytical model is needed.

For statistic modeling of the thickening as functions of six parameters there was used an interactive second order polynomial model, equation 2.

The coefficients of the equation 2 were determined based on the experimental data applying a computer program [1, 8, 9]. The all 48 coefficients are given in table 4.

$$y = b_o + b_1 r_{so} + b_2 r_v + b_3 \propto_{ro} + b_4 \propto_s + b_5 \propto_d + b_6 l + b_{11} r_{so}^2 + b_{22} r_v^2 + b_{33} \propto_{ro}^2 + b_{44} \propto_s^2 + b_{55} \propto_d^2 + b_6 l^2 + b_{12} r_{so} r_v + b_{13} r_{so} \propto_{ro} + b_{14} r_{so} \propto_s + b_{15} r_{so} \propto_d + b_{16} r_{so} l + b_{23} r_v \propto_{ro} + b_{24} r_v \propto_s + b_{25} r_v \propto_d + b_{26} r_v l + b_{34} \propto_{ro} \propto_s + b_{35} \propto_{ro} \propto_d + b_{36} \propto_{ro} l + b_{45} \propto_s \propto_d + b_{46} \propto_s l + b_{56} \propto_d l + b_{123} r_{so} r_v \propto_{ro} + b_{124} r_{so} r_v \propto_s + b_{125} r_{so} r_v \propto_d + b_{126} r_{so} r_v l + b_{134} r_{so} \propto_{ro} \propto_s + b_{135} r_{so} \propto_{ro} \propto_d + b_{136} r_{so} \propto_{ro} l + b_{145} r_{so} \propto_s \propto_d + b_{146} r_{so} \propto_s l + b_{156} r_{so} \propto_d l + b_{234} r_v \propto_{ro} \propto_s + b_{235} r_v \propto_{ro} \propto_d + b_{236} r_v \propto_{ro} l + b_{245} r_v \propto_s \propto_d + b_{246} r_v \propto_s l + b_{256} r_v \propto_d l + b_{345} \propto_{ro} \propto_s \propto_d + b_{346} \propto_{ro} \propto_s l + b_{356} \propto_{ro} \propto_d l + b_{456} \propto_s \propto_d l \quad (2)$$

Table 4

Model coefficients and their significance

Coefficient		PM_{bi}	F_{cs}	$F_{T[1;52;(1-\alpha)\%]}$		Coefficient		PM_{bi}	F_{cs}	$F_{T[1;52;(1-\alpha)\%]}$	
				α						α	
Symbol	Value			0,05	0,01	Symbol	Value			0,05	0,01
				4,023	7,172					4,023	7,172
b_0	0.28129	2.90	22110.27	√	√	b_{36}	0.0004057	0.80	6084.14	√	√
b_1	-0.01979	-1.91	-14591.09	√	√	b_{45}	-0.0005348	-0.13	-1008.03	√	√
b_2	-0.03250	-1.27	-9693.21	√	√	b_{46}	-0.0068878	-1.34	-10209.37	√	√
b_3	-0.00889	-4.53	-34518.24	√	√	b_{56}	-0.0066304	-1.29	-9865.45	√	√
b_4	0.00535	0.27	2062.17	√	√	b_{123}	-5.34E-05	-0.97	-7396.64	√	√
b_5	0.00028	0.01	109.54	√	√	b_{124}	0.0001155	0.21	1583.69	√	√
b_6	0.04802	1.91	14580.19	√	√	b_{125}	-3.48E-05	-0.06	-478.43	√	√
b_{11}	0.00046	0.48	3652.36	√	√	b_{126}	0.0001849	0.26	2004.46	√	√
b_{22}	-0.00241	-0.38	-2903.48	√	√	b_{134}	-7.98E-06	-0.19	-1424.70	√	√
b_{33}	-8.07E-06	-0.22	-1668.29	√	√	b_{135}	-1.48E-05	-0.35	-2651.99	√	√
b_{44}	-0.00027	-0.08	-587.20	√	√	b_{136}	-1.36E-05	-0.25	-1920.68	√	√
b_{55}	-5.63E-05	-0.02	-120.63	√	√	b_{145}	5.57E-05	0.13	984.80	√	√
b_{66}	0.00462	0.76	5807.50	√	√	b_{146}	0.000271	0.50	3784.31	√	√
b_{12}	0.001653	0.61	4631.07	√	√	b_{156}	0.000164	0.30	2296.05	√	√
b_{13}	0.000409	1.96	14902.73	√	√	b_{234}	-7.48E-05	-0.71	-5393.20	√	√
b_{14}	-0.00104	-0.49	-3756.44	√	√	b_{235}	-5.66E-05	-0.54	-4096.37	√	√
b_{15}	9.61E-05	0.05	348.04	√	√	b_{236}	-5.98E-05	-0.45	-3412.26	√	√
b_{16}	-0.00367	-1.37	-10466.66	√	√	b_{245}	5.88E-05	0.06	419.47	√	√
b_{23}	0.00153	2.96	22575.02	√	√	b_{246}	-2.95E-05	-0.02	-166.30	√	√
b_{24}	0.00186	0.36	2718.21	√	√	b_{256}	0.000785	0.58	4440.09	√	√
b_{25}	-0.00079	-0.15	-1160.24	√	√	b_{345}	-3.65E-05	-0.45	-3401.52	√	√
b_{26}	0.0007	0.12	908.06	√	√	b_{346}	1.35E-05	0.13	986.96	√	√
b_{34}	0.000543	1.36	10338.57	√	√	b_{356}	-2.65E-05	-0.26	-1950.47	√	√
b_{35}	0.00068	1.71	12995.05	√	√	b_{456}	0.000257	0.25	1868.56	√	√

The relative deviations between the calculated and numerical simulation values of thickening, the 95% confidence intervals for model predicted answers and the Δ predictive errors are shown in table 5. Statistical analysis was performed with codified variables model.

Table 5

Results of the statistical analysis

Exp. no.	Thickening [%]	$\widetilde{Thicke} - ning$ [%]	Error Δ [%]	The 95% confidence intervals [%]	Exp. no.	Thickening [%]	$\widetilde{Thicke} - ning$ [%]	Error Δ [%]	The 95% confidence intervals [%]
1	0.107	0.1066	-10.21	0,088 ÷ 0,125	51	0.189	0.1889	0.074	0,170 ÷ 0,207
2	0,062	0.0569	-7.15	0,038 ÷ 0,075	52	0.127	0.1249	1.67	0,106 ÷ 0,143
3	0.100	0.1011	-2.60	0,082 ÷ 0,119	53	0.143	0.1512	-5.44	0,133 ÷ 0,169
4	0.059	0.0604	-5.23	0,042 ÷ 0,079	54	0.093	0.0920	1.03	0,074 ÷ 0,110
5	0.029	0.0477	3.62	0,029 ÷ 0,066	55	0.185	0.1870	-1.04	0,168 ÷ 0,205
6	0.046	0.0393	2.14	0,020 ÷ 0,057	56	0.113	0.1126	0.37	0,094 ÷ 0,130
7	0.101	0.0897	5.76	0,071 ÷ 0,108	57	0.131	0.1330	-1.51	0,114 ÷ 0,151
8	0.062	0.0610	-1.66	0,042 ÷ 0,079	58	0.084	0.0758	10.77	0,057 ÷ 0,094
9	0.106	0.1045	-6.57	0,086 ÷ 0,123	59	0.155	0.1507	2.82	0,132 ÷ 0,169
10	0.049	0.0491	-6.37	0,030 ÷ 0,067	60	0.098	0.1154	-15.04	0,097 ÷ 0,133
11	0.104	0.1005	23.60	0,082 ÷ 0,118	61	0.114	0.1239	-7.96	0,105 ÷ 0,142
12	0.059	0.0618	4.34	0,043 ÷ 0,080	62	0.077	0.0775	-0.62	0,059 ÷ 0,095
13	0.073	0.0743	-8.71	0,056 ÷ 0,092	63	0.140	0.1409	-0.63	0,122 ÷ 0,159
14	0.057	0.0522	-3.66	0,033 ÷ 0,070	64	0.090	0.0872	3.21	0,068 ÷ 0,105
15	0.093	0.0961	2.51	0,077 ÷ 0,114	65	0.222	0.2011	10.38	0,184 ÷ 0,217
16	0.062	0.0617	-4.70	0,043 ÷ 0,080	66	0.065	0.0780	-16.71	0,061 ÷ 0,094
17	0.103	0.1065	5.81	0,088 ÷ 0,124	67	0.074	0.0626	18.20	0,046 ÷ 0,079
18	0.058	0.0588	-0.38	0,040 ÷ 0,077	68	0.093	0.0966	-3.68	0,080 ÷ 0,113
19	0.089	0.0933	-3.48	0,074 ÷ 0,111	69	0.099	0.0985	0.51	0,082 ÷ 0,114
20	0.062	0.0521	-7.43	0,034 ÷ 0,070	70	0.079	0.0717	10.23	0,055 ÷ 0,088
21	0.097	0.0824	-0.72	0,064 ÷ 0,100	71	0.112	0.1085	3.23	0,092 ÷ 0,124
22	0.055	0.0613	-3.60	0,043 ÷ 0,079	72	0.078	0.0737	5.87	0,057 ÷ 0,0901
23	0.093	0.1002	11.82	0,082 ÷ 0,118	73	0.113	0.1110	1.81	0,094 ÷ 0,127
24	0.055	0.0565	5.96	0,038 ÷ 0,074	74	0.088	0.0822	7.08	0,065 ÷ 0,098
25	0.089	0.0939	-10.55	0,075 ÷ 0,112	75	0.047	0.0558	-15.82	0,039 ÷ 0,072
26	0.049	0.0473	-3.67	0,028 ÷ 0,065	76	0.236	0.2193	7.60	0,202 ÷ 0,235
27	0.086	0.0842	-0.02	0,065 ÷ 0,102	77	0.089	0.0980	-9.17	0,093 ÷ 0,102
28	0.055	0.0520	-4.06	0,033 ÷ 0,070	78	0.088	0.0980	-10.19	0,093 ÷ 0,102
29	0.078	0.0793	-1.25	0,060 ÷ 0,097	79	0.088	0.0980	-10.19	0,093 ÷ 0,102
30	0.048	0.0514	0.07	0,033 ÷ 0,069	80	0.088	0.0980	-10.19	0,093 ÷ 0,102
31	0.074	0.0790	1.66	0,060 ÷ 0,097	81	0.08	0.0980	-18.35	0,093 ÷ 0,102
32	0.045	0.0364	-5.44	0,018 ÷ 0,054	82	0.081	0.0980	-17.34	0,093 ÷ 0,102
33	0.218	0.2089	1.03	0,190 ÷ 0,227	83	0.087	0.0980	-11.26	0,093 ÷ 0,102
34	0.107	0.1172	-1.04	0,098 ÷ 0,135	84	0.116	0.0980	18.38	0,093 ÷ 0,102
35	0.207	0.2149	0.37	0,196 ÷ 0,233	85	0.099	0.0980	1.03	0,093 ÷ 0,102
36	0.143	0.1395	-1.51	0,121 ÷ 0,157	86	0.096	0.0980	-2.03	0,093 ÷ 0,102
37	0.152	0.1595	10.77	0,141 ÷ 0,177	87	0.098	0.0980	0	0,093 ÷ 0,102
38	0.107	0.1011	2.82	0,082 ÷ 0,119	88	0.109	0.0980	11.23	0,093 ÷ 0,102
39	0.202	0.2028	-15.04	0,184 ÷ 0,221	89	0.115	0.0980	17.35	0,093 ÷ 0,102
40	0.127	0.1316	-7.96	0,113 ÷ 0,150	90	0.091	0.0980	-7.13	0,093 ÷ 0,102
41	0.156	0.1685	-0.62	0,150 ÷ 0,186	91	0.098	0.0980	0	0,093 ÷ 0,102
42	0.090	0.0907	-0.63	0,072 ÷ 0,109	92	0.094	0.0980	-4.07	0,093 ÷ 0,102
43	0.169	0.1753	3.21	0,156 ÷ 0,193	93	0.101	0.0980	3.07	0,093 ÷ 0,102
44	0.136	0.1216	10.38	0,103 ÷ 0,140	94	0.11	0.0980	12.25	0,093 ÷ 0,102
45	0.161	0.1519	-16.71	0,133 ÷ 0,170	95	0.108	0.0980	10.21	0,093 ÷ 0,102
46	0.089	0.0995	18.20	0,081 ÷ 0,117	96	0.089	0.0980	-9.17	0,093 ÷ 0,102
47	0.168	0.1744	-3.68	0,156 ÷ 0,192	97	0.105	0.0980	7.15	0,093 ÷ 0,102
48	0.117	0.1170	0.50	0,098 ÷ 0,135	98	0.097	0.0980	-1.01	0,093 ÷ 0,102
49	0.167	0.1741	10.23	0,155 ÷ 0,192	99	0.111	0.0980	13.27	0,093 ÷ 0,102
50	0.095	0.0962	3.23	0,077 ÷ 0,114	100	0.115	0.0980	17.35	0,093 ÷ 0,102

It is found that most of the measured responses fall into the 95% confidence intervals of responses predicted and measured responses erosion prediction are quite small, most of them with values below 10%.

The adequacy of a mathematical model consists in its capability to reproduce to an accepted accuracy the variation between measured characteristics and parameters of studied phenomena. It is established with the aid of statistical Fischer test and the results in case of proposed model and coefficients' significance are presented in Table 4.

Thus, for both level of confidence of 95% and 99%, the model is adequate, and all 48 regression coefficients are significant. The relative deviations between the calculated and numerical simulation values of thickening parameter, as well as the confidence intervals for thickening parameter are acceptable.

Some of the 3D graphics for relationships between thickening and the six mentioned parameters are shown in figures 9…14. In these graphics there were considered, one after the other, the relationship between the thickening and two of the parameters, the other four being at the medium value of its variation field.

Based on the significance indicators of the regression coefficients, an accurate analyze and ranking of the independent variables can be achieved. Thus (see Figures 9…14), from the point of view of influence intensity on thickening parameter, the independent variables are in the following order: wide of the flanged wall, fillet radius in vertical plane, fillet radius in horizontal plane, connection angle between the lateral side walls, bend angle between the left hand side wall of the part and normal to the surface of the part, bend angle between the right hand side wall of the part and normal to the surface of the part; the first three variables present a higher influence intensity than the last ones.

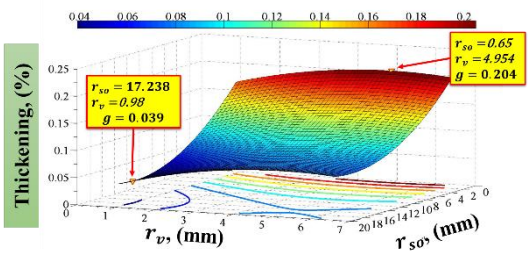

Fig. 9. Dependence of thickening on fillet radius in horizontal plane, r_{so}, and fillet radius in vertical plane, r_v

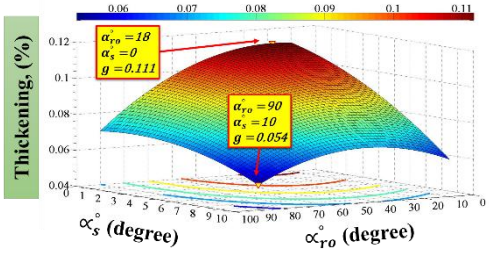

Fig. 10. Dependence of thickening on connection angle between the lateral side walls, α°_{ro}, and bend angle between the left hand side wall of the part and normal to the surface of the part, α°_{s}

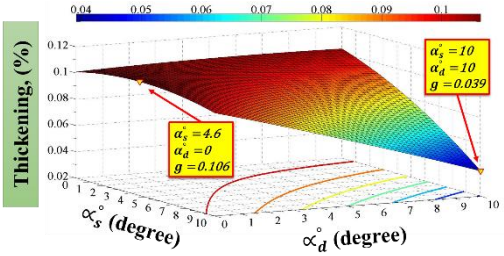

Fig. 11. Dependence of thickening on bend angle between the right hand side wall of the part and normal to the surface of the part, α_d°, and bend angle between the left hand side wall of the part and normal to the surface of the part, α_s°

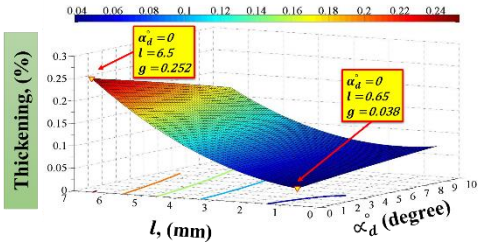

Fig. 12. Dependence of thickening on bend angle between the right hand side wall of the part and normal to the surface of the part, α_d°, and wide of the flanged wall, l

Based on analytical model determined, relation 2, in table 6 are given recommendations for choosing of geometrical characteristics for the parts with thickness of 0,65 mm, so that the maximum value allowable of the thickening does not exceed 1%, the value of the fillet radius in vertical plane, r_v, to be as small as possible (2 mm), the values of the angles between the both side wall of the part and normal to the surface of the part to be 90º and value of the wide of the flanged wall, l, to be as high as possible in the above conditions.

Table 6

Geometrical characteristics of shrink flanging part for thickness 0.65 mm and maximum admissible thickening 1%

Geometrical characteristics of the part						Thickening (%)	Thickness, g (mm)
r_{so} (mm)	r_v (mm)	α_{ro}° (degree)	α_s° (degree)	α_d° (degree)	l (mm)		
8 – 10	2	60	8	8	5	0,093 – 0.079	0,590 – 0.599
10.2 - 12	2	60	8	8	5	0,078 – 0.069	0,599 – 0.605
12.2 - 14	2	60	8	8	5	0.069 – 0.064	0.0605 – 0.609
14.2 – 15.4	2	60	8	8	5	0.064 – 0.062	0.609 – 0.610

5. Conclusions

Some relevant conclusions, concerning the thickening of the shrink flanging parts obtained in the above conditions, important for industrial applications and theoretical considerations, can be deducted.

The analytical model of the thickening is adequate, being utilizable for determination of the optimum cold plastic deformation conditions.

The model also allows to study the influence of those parameters on thickening and to determine the best conditions for its maximum acceptable value.

To obtain parts with an acceptable thickening of the flanged walls, four parameters must have values to the upper limits of the ranges of the studied, table 1,

respectively, fillet radius in horizontal plane, connection angle between the lateral side walls, bend angle between the left hand side wall of the part and normal to the surface of the part, bend angle between the right hand side wall of the part and normal to the surface of the part, while the other two parameters, namely, fillet radius in vertical plane and wide of the flanged wall it have values to the lower limit of the ranges of the studied.

Using numerical models can acquire data that can be the basis for optimization of the constructive characteristics of parts obtained by cold plastic deformation.

The numerical model used has a good flexibility based on the possibility to easy change geometrical and material parameters of the specimen and on its construction: rigid bodies group, on a side, and deformable material, to another side.

Hence, finite element method is a very important, accurate and vital tool for better and efficient design of shrink flanging process.

R E F E R E N C E S

[1] *C. Draghici, F. Mihaila*, Feasibility analysis of flanged holes with support of numerical simulation, "International journal of advancements in mechanical and aeronautical engineering", **volume 3**, issue1, [ISSN 2372-4153], 18 April, 2016, pp. 126 - 130

[2] Automotive steel design manual, revision 6.1, august 2002, American Iron and Steel Institute & auto/steel partnership, pp. 4.1-5

[3] *Gh., Sindila & CO*, Tehnologii de fabricare prin deformare plastica la rece, Editura Bren, Bucuresti 2009, ISBN 978-973-648-871-9

[4] *C. Ciocardia, FL. Draganescu, GH. Sindila, Craita Carp-Ciocardia si C. Parvu*, Tehnologia presarii la rece, Editura Didactica si Pedagogica, R.A., Bucuresti 1991, ISBN 973-30-2314-0, pp. 238 – 240

[5] *V. P. Romanovski*, Ștanțarea și matrițarea la rece (traducere din limba rusă), Editura tehnică, București, 1970, pp. 334

[6] *Ivana Suchy*, Handbook of Die Design, Second edition, McGraw-Hill , ISBN 0-07-146271-6

[7] *Yogesh Dewang, M. S. Hora and S. K. Panthi*, Review on finite element analysis of sheet metal stretch flanging process, ARPN Journal of Engineering and Applied Sciences, **vol. 9**, no. 9, September 2014, ISSN 1819-6608, pp. 1565 – 1579, www.arpnjournals.com

[8] *M.Gheorghe et al*, Algorithm and Computer Program for the Determination of Multivariable Regression Function, Bulletin of Polytechnic Institute of Bucharest, **vol. XLVI – XLVII**, 1984 - 1985 (in Romanian), (1985)

[9] *C. Draghici*, Statistical modelling of the spring back behavior for bending of V-shaped parts from common sheet metal, International Conference on Structural, Mechanical and Materials Engineering (ICSMME 2015), ISBN (on-line): 978-94-6252-144-5, ISSN 2352-5401 **volume 19**, doi:10.2991/icsmme-15.2015.25

[10] Product Catalogue from ArcelorMittal, File reference: B3.1, Cold Rolled Steel Sheet for Drawing and Forming EN 10130 DC01 ÷ DC06, https://flatsteel.arcelormittalsa.com/ fspcatalogue/DataSheets/UnCoated/ Web_datasheet_b3.1.pdf, on July 30, 2016